# FAMPKα1 deficiency suppresses brown adipogenesis in favor of fibrogenesis during brown adipose tissue development

**Junxing Zhao**[a,b], **Qiyuan Yang**[b], **Lupei Zhang**[b,d], **Xingwei Liang**[b], **Xiaofei Sun**[c], **Bo Wang**[b], **Yanting Chen**[b], **Meijun Zhu**[c], and **Min Du**[a,b,*]

[a]Department of Animal Sciences and Veterinary medicine, Shanxi Agricultural University, Taigu, Shanxi, 030800, China

[b]Department of Animal Sciences, Washington State University, Pullman, WA, 99164, US

[c]School of Food Science, Washington State University, Pullman, WA, 99164, US

[d]Institute of Animal Science, Chinese Academy of Agricultural Sciences, Beijing, 100193, China

## Abstract

Brown adipose tissue (BAT) dissipates energy for thermogenesis which reduces or prevents obesity and metabolic dysfunction. AMP-activated protein kinase (AMPK) is a master regulator of energy metabolism and its activity is inhibited in the developing BAT due to obesity. We previously found that AMPK is required for brown fat development and thermogenic function, but the non-brown adipogenic differentiation of progenitor cells due to AMPKα1 deficiency has not been defined. We found that, *in vivo*, the thermogenic capacity and morphology of BAT were compromised due to AMPK deficiency, which was correlated with decreased progenitor density in BAT. In addition, the expression of fibrogenic markers was higher in AMPK deficient compared to wild-type mice. Furthermore, we transplanted AMPKα1 wild-type (WT) and floxed BAT into the same recipient mice; following tamoxifen induced AMPKα1 knockout in floxed BAT, the fibrogenesis was enhanced compared to WT mice. Taken together, our data demonstrated that AMPKα1 deficiency suppressed brown adipogenesis in favor of fibrogenesis during BAT development.

### Keywords

Brown adipose tissue; AMPKα1; Fibrogenesis; Thermogenesis; Progenitor cells

## 1. Introduction

Brown adipose tissue (BAT) is originated from precursors in the dermomyotome that express Engrailed-1 (En1) and myogenic factor 5 (Myf5) [1]. BAT dissipates energy for

*Correspondence: min.du@wsu.edu.

**Publisher's Disclaimer:** This is a PDF file of an unedited manuscript that has been accepted for publication. As a service to our customers we are providing this early version of the manuscript. The manuscript will undergo copyediting, typesetting, and review of the resulting proof before it is published in its final citable form. Please note that during the production process errors may be discovered which could affect the content, and all legal disclaimers that apply to the journal pertain.

thermogenesis, and its content gradually decreases with aging [2]. BAT sizes in people with obesity are smaller [3], and lower metabolic activity of BAT is associated with insulin resistance and type 2 diabetes [4, 5]. Thus, activation of BAT function provides a feasible approach against T2D and obesity [6]. However, despite intense interest, the molecular mechanisms contributing to reduced BAT activity that occurs with obesity and diabetes are not fully understood.

The AMP-activated protein kinase (AMPK) is a conserved Serine/Threonine protein kinase that contains a catalytic subunit α and two regulatory subunits β and γ, and the α subunit has two isoforms α1 and α2 [7]. AMPK is a key mediator in cellular and whole-body energy balance by phosphorylating key enzymes, transcriptional activators and inhibitors [8]. Obesity, chronic inflammation and insulin resistance reduce AMPK activity [9], which correlates with incidences of metabolic diseases [10].

Recently, AMPK is proposed to regulate BAT thermogenic function indirectly via altering adrenergic nervous system in adults [11, 12]. Moreover, in the absence of AMPK activity, white adipose tissue becomes resistant to β-adrenergic-stimulated browning and thermogenesis [13]. Recently, our study shows that AMPK stimulates brown adipogenesis via facilitating DNA demethylation in the *Prdm16* promoter and its expression, and AMPK deficiency dramatically reduces neonatal BAT size and thermogenesis [14]. However, the non-brown adipogenic differentiation of progenitor cells due to AMPK deficiency has not been defined. Because AMPK α1 isoform is predominant in BAT [15], we hypothesized that AMPKα1 stimulates brown adipogenic differentiation of progenitor cells, and in the absence of AMPK activity, progenitor cells develop into fibrogenic cells instead of brown adipocytes.

## 2. Material and Methods

### 2.1 Care and use of animals

Animal studies were conducted according to the protocol approved by the Institute of Animal Use and Care Committees (IAUCC) at Washington State University. The constitutive *Prkaa1* and *Prkaa1* knockout (KO), and *Prkaa1*$^{\text{flox/flox}}$ mice were prepared as previously described [14]. To achieve *Prkaa1* conditional KO, Rosa26-Cre mice (Stock No: 004847, Jackson Lab, Bar Harbor, Maine, US) were crossed with *Prkaa1*$^{\text{flox/flox}}$ mice (Stock no: 014141) to obtain Rosa26$^{\text{Cre}}$/*Prkaa1* mice [16], and AMPK KO was induced by tamoxifen injection (75 μg/g body weight). For cold stimulation, mice were housed at either 4 °C or 22 °C with 12-h light/12-h dark cycles.

### 2.2 Histochemical, immunohistochemical and Masson Trichrome Staining

Brown adipose tissues fixed by 4% PFA (pH 7.4) were serially dehydrated in ethanol and xylene, and embedded in paraffin. Embedded samples were sectioned at 5 μm by microtome (Leica, German). Then, sections were dewaxed and rehydrated serially by incubation with xylene and different concentrations of ethanol. After that, sections were subjected to either hematoxylin & eosin staining, immunohistochemical staining or trichrome staining for histological examination. For immunofluorescence staining, antigen retrieval was performed by submerging in 0.01 M sodium citrate (pH 6.0) and boiled for 20 min in a microwave

oven. Then, BAT sections were subjected to immunofluorescence staining (UCP1, 1:200, Santa Cruz, CA, sc-28766). For Masson Trichrome staining of collagen, rehydrated tissue sections were stained as described in the kit instruction (HT15-1KT, Sigma-Aldrich, St louis, MO). Images were taken under EVOS® Cell Imaging Systems (Mill Creek, WA, US).

### 2.3 Real-time Quantitative PCR (RT-qPCR)

Total RNA was extracted using Trizol reagent (Sigma, Saint Louis, MO, USA) followed by DNase I (#M0303s, New England Biolabs, Ipswich, MA) digestion. Concentration and the integrity of RNA samples were determined by both NanoDrop ND-2000 instrument (Nanodrop Instruments, Delaware, USA) and by electrophoresis using 2% agarose gel. Total 1 μg RNA was used for cDNA synthesis using a reverse transcription kit (Bio-Rad, Hercules, CA, US), with RT-qPCR performed using the CFX RT-PCR detection system (Bio-Rad, Hercules, California, US) and a SYBR Green RT-PCR kit (Bio-Rad, Hercules, CA, US). Relative mRNA content was normalized to the *18S rRNA* gene. Primer sets used are listed in Table 1.

### 2.4 Flow Cytometry

Mouse primary brown fat vascular stromal fraction cells (BSVs) were freshly prepared [14], blocked using anti-mouse CD16/CD32 antibody (101320, Biolegend, SanDiego, CA, US) and then stained with anti-mouse CD45 (103111, Biolegend) and anti-mouse Sca-1 (45-5981, eBioscience, SanDiego, CA, US) antibodies. Brown Sca-1$^+$/CD45$^-$/Lin$^-$ progenitor cells were sorted on FACSaria (BD Biosciences, San Jose, CA) and analyzed by FlowJo software (Treestar Inc., San Carlos, CA).

### 2.5 Oxygen consumption assays

BATs were isolated from either WT or AMPKα1 KO mice, and 20 mg of tissue slice was placed in a respiration buffer (2% BSA, 1.1 mM Sodium pyruvate and 25 mM glucose in PBS). Oxygen consumption was measured using an Orion Dissolved Oxygen platform (Thermo Scientific, Waltham, MA, US) for approximately 25 min [17].

### 2.6 Brown fat transplantation

3-week-old C57BL/6 recipient mice were anesthetized by isoflurane inhalation. BAT was removed from the interscapular region of neonatal mice (both *Prkaa1*$^{flox/flox}$: *Cre*$^{-/-}$ mice and *Prkaa1* $^{flox/flox}$: *Cre*$^{+/-}$), and about 10 mg donor BATs were transplanted into the left and right subcutaneous region, adjacent to the endogenous interscapular fat pads of recipient mice, respectively. Three days after transplantation, recipient mice were injected with tamoxifen daily for four days to induce *Prkaa1* KO in transplanted *Prkaa1*$^{flox/flox}$: *Cre*$^{+/-}$ BAT [14].

### 2.7 Thermal imagining

Thermo-images were taken using an E6 Thermal Imaging Infrared Camera (FLIR Systems, Boston, MA).

**2.8 Transmission electron microscope (TEM) and Scanned electron microscope (SEM)**

The protocols were conducted as previously described [14].

**2.9 Statistical analyses**

Statistical analysis was performed using the Graphpad Prism 7 software package (Monrovia, CA, USA). The data are expressed as the mean ± SEM and analyzed using Student's *t*-test or one way ANOVA (for multiple comparison) where appropriate. $P < 0.05$ was considered statistically significant and $P < 0.10$ was considered as a trend.

## 3. Results

### 3.1 AMPKα1 ablation impairs brown adipogenesis

The BAT mass was smaller in *Prkaa1* constitutive knockout (KO) mice than wild-type (WT) mice (Fig. 1A). The dorsal interscapular temperature (DIT) of *Prkaa1* KO mice was convincingly lower than that of WT mice ($P < 0.001$, Fig. 1B and 1C). Supportively, the same phenomenon was observed in conditional KO mice induced by tamoxifen after birth (Fig. 1D and 1E). The AMPKα1$^{-/-}$ BAT had a lower rate of oxygen consumption at weaning (Fig. 1F). Histologically, from E18.5 to postnatal 6 months of age, AMPKα1 deficient BAT had denser staining, suggesting less lipid accumulation (Fig. 1G), which was confirmed by scanning electron microscopic examination. The lipid droplets appeared smaller and uneven in AMPKα1$^{-/-}$ mice (Fig. 1H). Consistently, less UCP1 was detected by immunohistochemical staining (Fig. 1I). These data suggest that AMPKα1 deficiency leads to long-term impairment on the structure and thermogenic function of BAT.

### 3.2 AMPKα1 ablation inhibits brown adipogenesis but facilitates fibrogenesis in BAT

A subpopulation of cells (Sca-1$^+$/CD45$^-$) residing in brown fat was identified as brown progenitor cells [18]. Unexpectedly, the frequency of Sca-1$^+$/CD45$^-$ progenitor cells from neonatal BAT was higher in *Prkaa1* KO compared to WT BAT at birth, which could be due to weakened *Prdm16* expression in BAT progenitor cells resulting in blocked brown adipogenesis and accumulation of progenitor cells (Fig. 2A and 2B). However, the population of progenitor cells became similar between WT and KO BAT at P4 (Fig. 2C and 2D). Supportively, transmission electron microscopic (TEM) observation confirmed impaired differentiation of progenitor cells in AMPKα1$^{-/-}$ BAT; many progenitor cells could not be differentiated into brown adipocytes possessing multilocular lipid droplets (Fig. 2E). Moreover, AMPKα1 ablation had negative effect on the formation of cristae of mitochondria and density of mitochondria (Fig. 2F). On the other hand, the mRNA expression of fibrogenic markers, including *P4HA*, *fibronectin* and *collagen1a*, was higher in BAT due to *Prkaa1* KO (Fig. 2G), showing enhanced fibrogenesis.

In addition, we examined BAT at P10, and similar impairment in lipid droplets and mitochondrial cristae were observed in AMPKα1$^{-/-}$ BAT (Fig. 3A). To further demonstrate whether there was enhanced fibrogenesis, we used trichrome staining to identify collagen. Higher amount of collagen was present in AMPKα1$^{-/-}$ BAT, confirming enhanced fibrogenesis (Fig. 3B). Such difference maintained in the BAT of 6-month-old mice, where the expression of fibrogenic markers was higher in AMPKα1$^{-/-}$ BAT (Fig. 3C). In addition,

we induced brown adipogenic differentiation of BSVs, and found that the expression of brown adipogenic markers was reduced in AMPKα1$^{-/-}$ deficient BSVs but the expression of fibrogenic markers was enhanced (Fig. 3D). In aggregate, these data show that AMPKα1 absence attenuates brown adipogenesis in favor of fibrogenesis in developing BAT.

### 3.3 AMPKα1$^{-/-}$ BAT has attenuated thermogenic functionality during cold stimulation

The primary function of BAT is to generate heat to maintain core temperature when exposed to cold [19]. When exposed to cold, the body surface temperature of *Prkaa1* KO mice was notably lower than that of WT mice (Fig. 4A), showing impaired thermogenesis. Furthermore, when treated with CL316,243, a β3-adreceptor agonist which specifically activates BAT thermogenesis, the body temperature of WT (*Prkaa1*$^{+/+}$) mice was substantially increased, which was not observed in *Prkaa1* KO mice, clearly showing the impairment of BAT function due to absence of AMPKα1 (Fig. 4B).

To conclusively establish the role of AMPK in BAT development, we conducted a BAT transplantation study, where neonatal BATs from both Rosa26$^{Cre}$/AMPKα1 floxed and Rosa26$^{Cre}$/WT mice were transplanted into the interscapular areas of the same recipient mice and, then, AMPKα1 KO was induced by tamoxifen. We found that AMPKα1 acute KO following transplantation decreased expression of brown adipogenic markers. Metformin administration increased both *UCP1* and *Cidea* mRNA expression in transplanted WT BAT, and such changes were not observed in AMPKα1$^{-/-}$ BAT (Fig. 4C). Consistently, the expression of fibrogenic markers, including P4HA and collagen1a was higher due to AMPK deficiency (Fig. 4D), further confirming that AMPK absence facilitated fibrogenesis in BAT.

## 4. Discussion

Brown adipose tissue is one of the most efficient organs to absorb glucose and clean lipids [20], and the attenuation of BAT thermogenic function not only compromises peripheral tissue insulin sensitivity but also has persistent negative impact on the whole body metabolism [21]. Obesity and type 2 diabetes are associated with impaired BAT functions [22] and decreased AMPK activity [23]. Thus, enhancing BAT development is a promising therapeutic strategy for preventing obesity and improving metabolic health [24–27].

Our recent study reveals that AMPKα1 is required for brown adipogenesis via regulation of *Prdm16* expression, and AMPK deficiency blocks brown adipogenic differentiation of progenitor cells [14], which raises an interesting question: what is the alternative destination of these progenitor cells which cannot undergo brown adipogenesis? Therefore, we traced the density and their differentiation of progenitor cells. Interestingly, the population of progenitor cells in BAT from neonatal mice was higher in AMPK KO compared to WT mice. One plausible explanation is that AMPK deficiency blocked brown adipogenesis leading to the accumulation of progenitor cells in neonatal BAT. To confirm, we examined ultramicroscopic structure of BAT, and the results showed presence of undifferentiated cells in BAT due to AMPK deficiency, consistent with the higher density of progenitor cells based on cell sorting. However, the population of progenitor cells became similar between WT and KO BAT at postnatal day 4, and at postnatal day 21 the density was higher in WT compared

to KO[14], showing the accelerated depletion of progenitor cells in the developing BAT due to AMPK deficiency. These data prompted us to further examine the non-brown adipogenic commitment of progenitor cells due to AMPK deficiency. Consistently, we found that, accompanying attenuated brown adipogenesis, fibrogenesis was enhanced. The expression of fibrogenic markers was higher in BAT with AMPK ablation, while that of thermogenic genes was reduced. These data are in agreement with our previous observations that obesity during early development enhances fibrogenesis in fetal skeletal muscle [28–30].

To rule out the systemic effects of AMPKα1 ablation, E18.5 fetal BAT was obtained from both Rosa26[Cre]/AMPKα1 floxed and Rosa26[Cre]/AMPK WT mice and transplanted into the same recipient mice. After transplantation, the AMPKα1 ablation was induced in transplanted Rosa26[Cre]/AMPKα1 floxed BAT by tamoxifen, which did not affect AMPK in WT BAT. In alignment, the expression of *UCP1*, *Cox7a* and *Cidea* was dramatically suppressed in transplanted AMPKα1 KO BAT when compared to WT BAT. Metformin administration enhanced the expression of *UCP1* and *Cidea* in WT BAT but not in KO BAT. Our findings are consistent with accumulating evidences showing the promotional effects of AMPK activation on brown and beige adipogenesis [17, 31–34]. On the other side, the expression of fibrogenic markers was higher in transplanted BAT with AMPK deficiency. Because the transplanted WT and KO BAT developed under the same physiological condition (the same recipient mice) and AMPK KO was induced after transplantation, the difference in gene expression and fibrogenesis of transplanted BAT clearly showed that AMPKα1 deficiency enhances fibrogenesis but reduces brown adipogenesis of progenitor cells during BAT development. To the knowledge of authors, this is the first report showing enhanced fibrogenesis during BAT development due to AMPK deficiency.

In summary, AMPK deficiency reduces progenitor density and suppresses brown adipogenesis in favor of fibrogenesis. Thus, AMPK is an important target for promoting BAT development.

## Acknowledgments

## References

1. Kajimura S, Seale P, Spiegelman BM. Transcriptional control of brown fat development. Cell Metab. 2010; 11:257–262. [PubMed: 20374957]

2. Cypess AM, White AP, Vernochet C, Schulz TJ, Xue R, Sass CA, Huang TL, Roberts-Toler C, Weiner LS, Sze C. Anatomical localization, gene expression profiling and functional characterization of adult human neck brown fat. Nat Med. 2013; 19:635–639. [PubMed: 23603815]

3. van Marken Lichtenbelt WD, Vanhommerig JW, Smulders NM, Drossaerts JM, Kemerink GJ, Bouvy ND, Schrauwen P, Teule GJ. Cold-activated brown adipose tissue in healthy men. New Engl J Med. 2009; 360:1500–1508. [PubMed: 19357405]

4. Chondronikola M, Volpi E, Børsheim E, Porter C, Annamalai P, Enerbäck S, Lidell ME, Saraf MK, Labbe SM, Hurren NM. Brown adipose tissue improves whole-body glucose homeostasis and insulin sensitivity in humans. Diabetes. 2014; 63:4089–4099. [PubMed: 25056438]

5. Blondin DP, Labbé SM, Noll C, Kunach M, Phoenix S, Guérin B, Turcotte ÉE, Haman F, Richard D, Carpentier AC. Selective impairment of glucose, but not fatty acid or oxidative metabolism in brown adipose tissue of subjects with type 2 diabetes. Diabetes. 2015; 64:2388–2397. [PubMed: 25677914]

6. Dulloo AG. Translational issues in targeting brown adipose tissue thermogenesis for human obesity management. Ann N Y Acad Sci. 2013; 1302:1–10. [PubMed: 24138104]

7. Hardie DG, Hawley SA, Scott JW. AMP-activated protein kinase--development of the energy sensor concept. J Physiol. 2006; 574:7–15. [PubMed: 16644800]

8. Hoffman NJ, Parker BL, Chaudhuri R, Fisher-Wellman KH, Kleinert M, Humphrey SJ, Yang P, Holliday M, Trefely S, Fazakerley DJ. Global phosphoproteomic analysis of human skeletal muscle reveals a network of exercise-regulated kinases and AMPK substrates. Cell Metab. 2015; 22:922–935. [PubMed: 26437602]

9. Steinberg GR, Michell BJ, van Denderen BJ, Watt MJ, Carey AL, Fam BC, Andrikopoulos S, Proietto J, Gorgun CZ, Carling D, Hotamisligil GS, Febbraio MA, Kay TW, Kemp BE. Tumor necrosis factor alpha-induced skeletal muscle insulin resistance involves suppression of AMP-kinase signaling. Cell Metab. 2006; 4:465–474. [PubMed: 17141630]

10. Eng GS, Sheridan RA, Wyman A, Chi MM, Bibee KP, Jungheim ES, Moley KH. AMP kinase activation increases glucose uptake, decreases apoptosis, and improves pregnancy outcome in embryos exposed to high IGF-I concentrations. Diabetes. 2007; 56:2228–2234. [PubMed: 17575082]

11. Whittle AJ, Carobbio S, Martins L, Slawik M, Hondares E, Vazquez MJ, Morgan D, Csikasz RI, Gallego R, Rodriguez-Cuenca S, Dale M, Virtue S, Villarroya F, Cannon B, Rahmouni K, Lopez M, Vidal-Puig A. BMP8B increases brown adipose tissue thermogenesis through both central and peripheral actions. Cell. 2012; 149:871–885. [PubMed: 22579288]

12. Martinez de Morentin PB, Gonzalez-Garcia I, Martins L, Lage R, Fernandez-Mallo D, Martinez-Sanchez N, Ruiz-Pino F, Liu J, Morgan DA, Pinilla L, Gallego R, Saha AK, Kalsbeek A, Fliers E, Bisschop PH, Dieguez C, Nogueiras R, Rahmouni K, Tena-Sempere M, Lopez M. Estradiol Regulates Brown Adipose Tissue Thermogenesis via Hypothalamic AMPK. Cell Metab. 2014; 20:41–53. [PubMed: 24856932]

13. Mottillo EP, Desjardins EM, Crane JD, Smith BK, Green AE, Ducommun S, Henriksen TI, Rebalka IA, Razi A, Sakamoto K. Lack of adipocyte AMPK exacerbates insulin resistance and hepatic steatosis through brown and beige adipose tissue function. Cell Metab. 2016; 24:118–129. [PubMed: 27411013]

14. Yang Q, Liang X, Sun X, Zhang L, Fu X, Rogers CJ, Berim A, Zhang S, Wang S, Wang B, Foretz M, Viollet B, Gang DR, Rodgers BD, Zhu MJ, Du M. AMPK/alpha-Ketoglutarate Axis Dynamically Mediates DNA Demethylation in the Prdm16 Promoter and Brown Adipogenesis. Cell Metab. 2016; 24:542–554. [PubMed: 27641099]

15. Daval M, Diot-Dupuy F, Bazin R, Hainault I, Viollet B, Vaulont S, Hajduch E, Ferré P, Foufelle F. Anti-lipolytic action of AMP-activated protein kinase in rodent adipocytes. J Biol Chem. 2005; 280:25250–25257. [PubMed: 15878856]

16. Fu X, Zhu M, Zhang S, Foretz M, Viollet B, Du M. Obesity impairs skeletal muscle regeneration through inhibition of AMPK. Diabetes. 2016; 65:188–200. [PubMed: 26384382]

17. Wang S, Liang X, Yang Q, Fu X, Rogers CJ, Zhu M, Rodgers BD, Jiang Q, Dodson MV, Du M. Resveratrol induces brown-like adipocyte formation in white fat through activation of AMP-activated protein kinase (AMPK) alpha1. Int J Obes (Lond). 2015; 39:967–976. [PubMed: 25761413]

18. Schulz TJ, Huang TL, Tran TT, Zhang H, Townsend KL, Shadrach JL, Cerletti M, McDougall LE, Giorgadze N, Tchkonia T, Schrier D, Falb D, Kirkland JL, Wagers AJ, Tseng YH. Identification of inducible brown adipocyte progenitors residing in skeletal muscle and white fat. Proc Natl Acad Sci USA. 2011; 108:143–148. [PubMed: 21173238]

19. Sidossis L, Kajimura S. Brown and beige fat in humans: thermogenic adipocytes that control energy and glucose homeostasis. J Clin Invest. 2015; 125:478–486. [PubMed: 25642708]

20. Townsend KL, Tseng YH. Brown fat fuel utilization and thermogenesis. Trends Endocrinol Metab TEM. 2014; 25:138–177. [PubMed: 24388149]

21. Yoneshiro T, Aita S, Matsushita M, Kameya T, Nakada K, Kawai Y, Saito M. Brown adipose tissue, whole-body energy expenditure, and thermogenesis in healthy adult men. Obesity. 2011; 19:13–16. [PubMed: 20448535]

22. Stanford KI, Middelbeek RJ, Townsend KL, An D, Nygaard EB, Hitchcox KM, Markan KR, Nakano K, Hirshman MF, Tseng YH. Brown adipose tissue regulates glucose homeostasis and insulin sensitivity. J Clin Invest. 2013; 123:215–223. [PubMed: 23221344]

23. Ruderman NB, Carling D, Prentki M, Cacicedo JM. AMPK, insulin resistance, and the metabolic syndrome. J Clin Invest. 2013; 123:2764–2772. [PubMed: 23863634]

24. Virtanen KA, Lidell ME, Orava J, Heglind M, Westergren R, Niemi T, Taittonen M, Laine J, Savisto NJ, Enerbäck S. Functional brown adipose tissue in healthy adults. N Engl J Med. 2009; 360:1518–1525. [PubMed: 19357407]

25. Nedergaard J, Bengtsson T, Cannon B. New powers of brown fat: fighting the metabolic syndrome. Cell Metab. 2011; 13:238–240. [PubMed: 21356513]

26. Bartelt A, Bruns OT, Reimer R, Hohenberg H, Ittrich H, Peldschus K, Kaul MG, Tromsdorf UI, Weller H, Waurisch C, Eychmuller A, Gordts PL, Rinninger F, Bruegelmann K, Freund B, Nielsen P, Merkel M, Heeren J. Brown adipose tissue activity controls triglyceride clearance. Nat Med. 2011; 17:200–205. [PubMed: 21258337]

27. Sacks H, Symonds ME. Anatomical locations of human brown adipose tissue: functional relevance and implications in obesity and type 2 diabetes. Diabetes. 2013; 62:1783–1790. [PubMed: 23704519]

28. Huang Y, Yan X, Zhao JX, Zhu MJ, McCormick RJ, Ford SP, Nathanielsz PW, Ren J, Du M. Maternal obesity induces fibrosis in fetal myocardium of sheep. Am J Physiol Endocrinol Metab. 2010; 299:E968–975. [PubMed: 20876759]

29. Huang Y, Yan X, Zhu MJ, McCormick RJ, Ford SP, Nathanielsz PW, Du M. Enhanced transforming growth factor-beta signaling and fibrogenesis in ovine fetal skeletal muscle of obese dams at late gestation. Am J Physiol Endocrinol Metab. 2010; 298:E1254–1260. [PubMed: 20371734]

30. Huang Y, Zhao JX, Yan X, Zhu MJ, Long NM, McCormick RJ, Ford SP, Nathanielsz PW, Du M. Maternal obesity enhances collagen accumulation and cross-linking in skeletal muscle of ovine offspring. PloS one. 2012; 7:e31691. [PubMed: 22348119]

31. Ko SC, Lee M, Lee JH, Lee SH, Lim Y, Jeon YJ. Dieckol, a phlorotannin isolated from a brown seaweed, Ecklonia cava, inhibits adipogenesis through AMP-activated protein kinase (AMPK) activation in 3T3-L1 preadipocytes. Environ Toxicol Pharmacol. 2013; 36:1253–1260. [PubMed: 24211593]

32. Lim H, Park J, Kim HL, Kang J, Jeong MY, Youn DH, Jung Y, Kim YI, Kim HJ, Ahn KS, Kim SJ, Choe SK, Hong SH, Um JY. Chrysophanic acid suppresses adipogenesis and Induces thermogenesis by activating AMP-Activated protein kinase alpha In vivo and In vitro. Front Pharmacol. 2016; 7:476. [PubMed: 28008317]

33. Lone J, Choi JH, Kim SW, Yun JW. Curcumin induces brown fat-like phenotype in 3T3-L1 and primary white adipocytes. J Nutr Biochem. 2016; 27:193–202. [PubMed: 26456563]

34. Xu Z, Liu J, Shan T. New roles of Lkb1 in regulating adipose tissue development and thermogenesis. J Cell Physio. 2016; 132:2296–2298.

35. Crane JD, Palanivel R, Mottillo EP, Bujak AL, Wang H, Ford RJ, Collins A, Blumer RM, Fullerton MD, Yabut JM, Kim JJ, Ghia JE, Hamza SM, Morrison KM, Schertzer JD, Dyck JR, Khan WI, Steinberg GR. Inhibiting peripheral serotonin synthesis reduces obesity and metabolic dysfunction by promoting brown adipose tissue thermogenesis. Nat med. 2014; 21:166–172. [PubMed: 25485911]

## Highlight

1.  The brown adipogenesis were compromised due to AMPK deficiency.

2.  AMPK deficiency was correlated with decreased progenitor cell density in BAT.

3.  The expression of fibrogenic markers was higher in AMPK deficient condition.

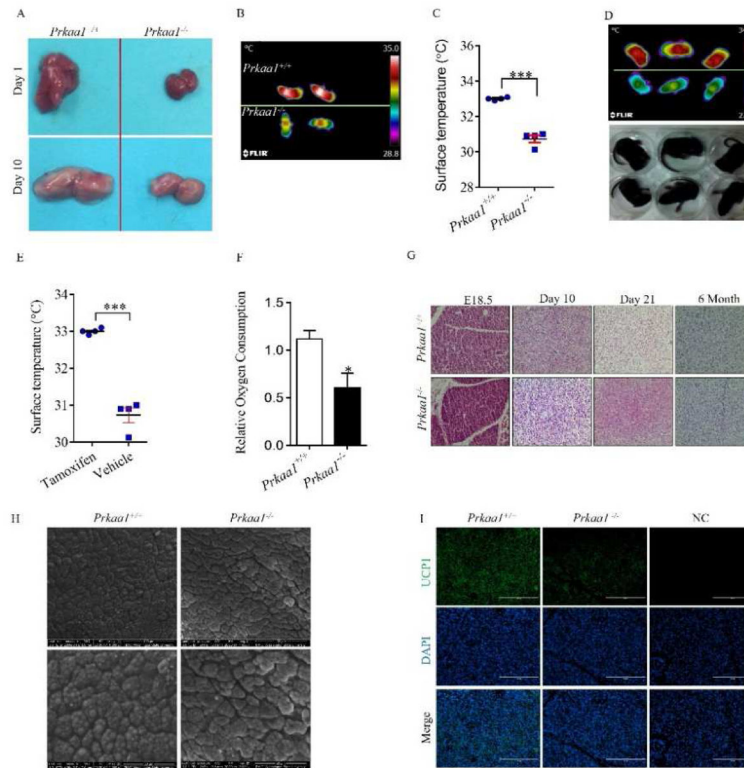4.  AMPK deficiency drives progenitor cells to fibrogenesis.

**Figure 1.**
AMPKα1 ablation impairs brown adipogenesis. (A) Interscapular BAT of wild-type (WT) and *Prkaa1* knockout (KO) at postnatal day 1 (P1) and P10. (B and C) Dorsal interscapular surface temperature of WT mice and *Prkaa1* KO mice at P4. (D and E) Infrared (up) and photographic (down) images of tamoxifen-induced conditional WT and *Prkaa1* KO mice at P7 (D), and quantification of skin surface temperature (E). (F) Relative oxygen consumption of BAT in WT and *Prkaa1* KO mice at P21. (G) Hematoxylin and eosin (H&E) staining of sections from the interscapular regions of WT and KO mice at E18.5, P10, P21 and 6 months of age. (H) Scanning electron microscopic images of BAT at P10 (2,000 ×). (I) Immunofluorescence staining for UCP1 of WT and KO BAT at P10. (*$P < 0.05$; **$P < 0.01$).
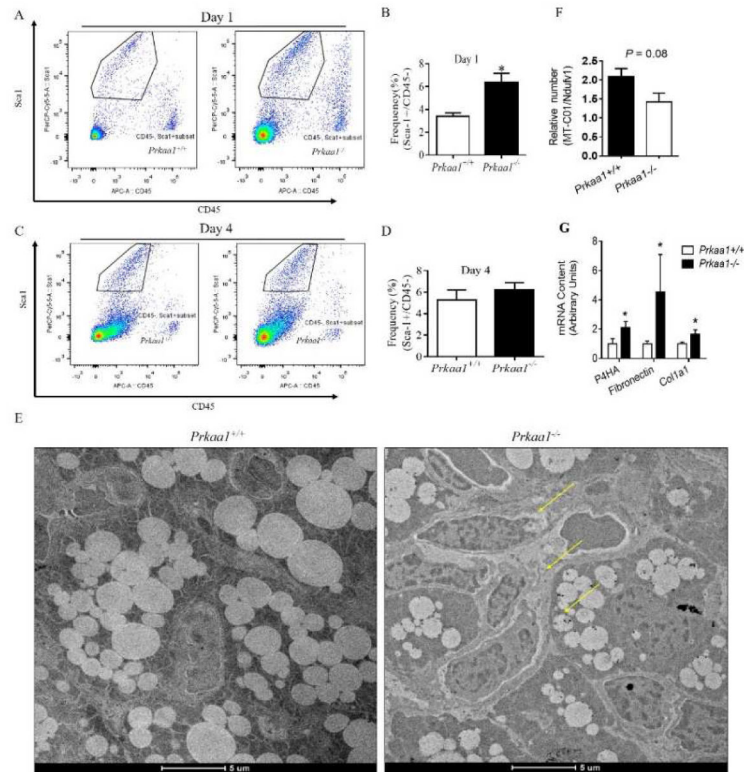
**Figure 2.**

*Prkaa1* KO suppresses BAT development through reducing proliferation of brown preadipocytes and exhaustion of stem cell pool. (A–D) Flow cytometry plots of brown progenitor cells from interscapular BAT of WT and KO mice at P1 and P4, with black cycles denoting the population of Lin⁻/Sca1⁺/CD45⁻ brown adipogenic progenitors (A and C) and quantification of progenitor cells (B and D). (E) Transmission electron microscopic examination at postnatal day P1. (F) Ratio of mitochondrial DNA levels in BAT from P1 WT and KO mice (Calculated based on the ratio of mitochondrial gene *MT-CO1* and nuclear gene *Ndufv1* by PCR). (G) mRNA expression of fibrogenic markers. (*$P < 0.05$).
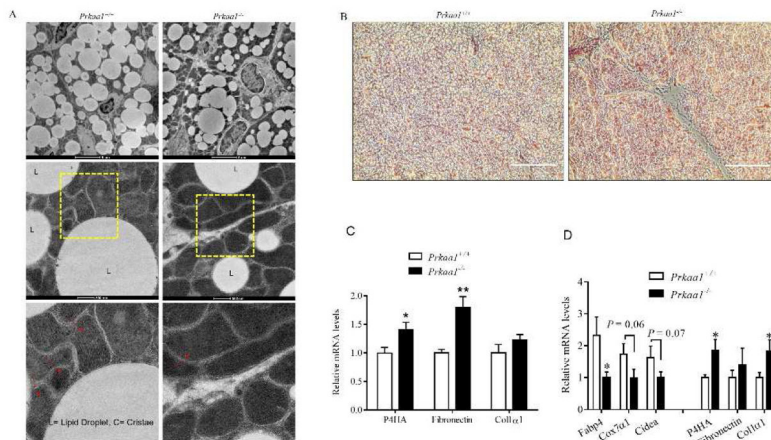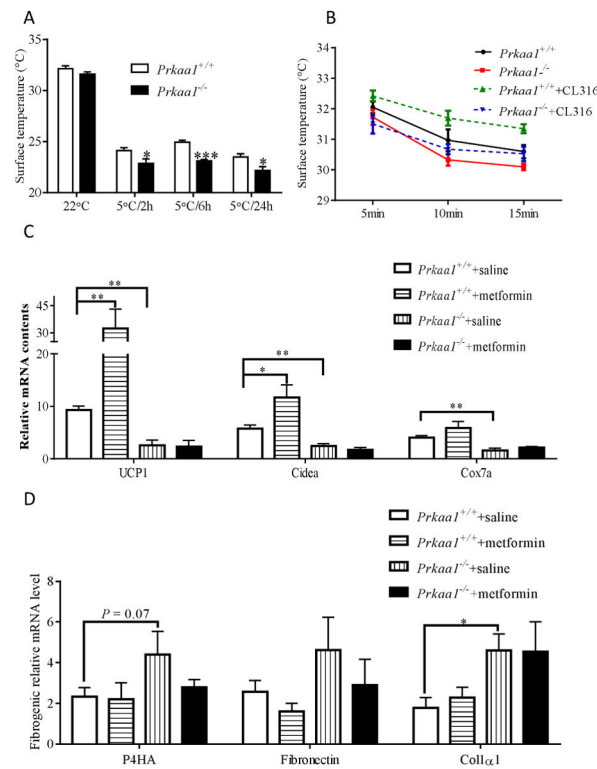
**Figure 3.**
*Prkaa1* KO facilitates fibrosis in BAT. (A) Transmission electron microscopic examination at P10. (B) Masson's trichrome staining was conducted between WT and KO mice at P10, data showed that *AMPKα1* KO induced collagen deposition. (C) Expression of brown fibrogenic markers in BAT of WT and *Prkaa1* KO mice at 6 months of age. (D) Expression of adipogenic and fibrogenic markers after 7 days of differentiation of WT and KO brown stromal vascular fibroblasts (BSVs). (*$P < 0.05$; **$P < 0.01$).

**Figure 4.**
AMPKα1⁻/⁻ mice impairs BAT function during cold stimulation. (A) Thermostasis (skin temperature) of *Prkaa1* KO mice (2 months old) was impaired due to cold exposure at 5°C for 2, 6, and 24 h. (B) Tracing interscapular region thermogenesis of anesthetized WT and *Prkaa1* KO mice at different check points after injection with saline or CL-316243 as previously described [35]. (C) mRNA expression in transplanted BATs. Data shows that metformin only enhances the expression of brown adipogenic markers in WT BAT, not in AMPKα1 ablated BAT. (D) mRNA expression of fibrosis markers in transplanted BATs. (\*$P < 0.05$; \*\*$P < 0.01$).

**Table 1**

Primer sequences for Real-time PCR

| Name | Sequence (5′–3′) |
|------|------------------|
| UCP1 | ACTGCCACACCTCCAGTCATT |
|      | CTTTGCCTCACTCAGGATTGG |
| Cidea | ATCACAACTGGCCTGGTTACG |
|       | TACTACCCGGTGTCCATTTCT |
| Fabp4 | CGACAGGAAGGTGAAGAGCATCATA |
|       | CATAAACTCTTGTGGAAGTCACGCCT |
| Cox7a | CAGCGTCATGGTCAGTCTGT |
|       | AGAAAACCGTGTGGCAGAGA |
| PGC-1α | AAGTGGTGTAGCGACCAATCG |
|        | AATGAGGGCAATCCGTCTTCA |
| Fibronectin | CACTGCAGAACCAGAGGAGG |
|             | TGAGCTTAAAGCCAGCGTCA |
| P4HA | TCAAGGACATGTCGGATGGC |
|      | TTCAGGATCTGGAAGATTCCCC |
| Collagen I a | TTCTCCTGGCAAAGACGGAC |
|              | CGGCCACCATCTTGAGACTT |
| Ndufv1 | CTTCCCCACTGGCCTCAAG |
|        | CCAAAACCCAGTGATCCAGC |
| MT-CO1 | TGCTAGCCGCAGGCATTAC |
|        | GGGTGCCCAAAGAATCAGAAC |
| 18 S | GTAACCCGTTGAACCCCATT |
|      | CCATCCAATCGGTAGTAGCG |